journal

J. Am. Ceram. Soc., **82** [11] 2943–47 (1999)

Effect of Sintering Aid Composition on the Processing of Si_3N_4/BN Fibrous Monolithic Ceramics

Rodney W. Trice*,† and John W. Halloran*

Materials Science and Engineering Department, University of Michigan, Ann Arbor, Michigan 48109-2136

Si_3N_4/BN fibrous monoliths were prepared with 4 wt% Y_2O_3 added as a sintering aid to the Si_3N_4. Residual carbon, present in the billet before hot-pressing, was shown to influence the final microstructure. The sintering aid glass, known to migrate into the BN cell boundaries during hot-pressing, was not sufficient in quantity to prevent premature shear failure when samples were tested in flexure. Increasing the hot-pressing temperature alleviated this problem. For flexure samples tested at 1400°C, fibrous monoliths fabricated with 4 wt% Y_2O_3 demonstrated linear-elastic loading behavior at a greater stress than fibrous monoliths fabricated with 6-wt%-Y_2O_3/2-wt%-Al_2O_3 sintering aids.

I. Introduction

THE unique flexural response of fibrous monoliths, consisting of strong cells of Si_3N_4 surrounded by weaker cell boundaries of BN, is a result of the submillimeter architecture engineered into the material.[1] Because ~80 vol% of fibrous monoliths are composed of Si_3N_4 cells, improvements in the refractoriness of this phase should improve the refractoriness of the composite material.

It is well-established that the sintering aids used to process Si_3N_4 profoundly affect its mechanical properties.[2,3] The sintering aids react with the thin layer of SiO_2 that surrounds each individual particle of Si_3N_4, forming an oxynitride liquid, which, upon cooling, forms an intergranular phase that is typically amorphous.[4,5] The composition of this intergranular phase strongly influences the mechanical properties of Si_3N_4 as temperature is increased.[6,7] Small amounts of Y_2O_3 added as sintering aid are known to produce very refractory hot-pressed Si_3N_4.[8] Y_2O_3-doped Si_3N_4, specifically NT-154, which contains ~4 wt% Y_2O_3 additions, has demonstrated excellent creep properties.[9–12]

Based on this understanding, it was hypothesized that the high-temperature flexure properties of fibrous monoliths could be improved by using only Y_2O_3 as a sintering aid in the cells of Si_3N_4. Thus, fabrication of 4-wt%-Y_2O_3–Si_3N_4/BN fibrous monoliths (4Y-FMs) was investigated. This paper describes several of the processing difficulties associated with fabricating this composition of fibrous monolith. The effect of varying the composition of sintering aids on the high-temperature mechanical properties is discussed by comparing 4Y-FMs with less-refractory 6-wt%-Y_2O_3–2-wt%-Al_2O_3–Si_3N_4/BN fibrous monoliths (6Y/2Al-FMs).

F. W. Zok—contributing editor

Manuscript No. 190140. Received May 29, 1998; approved April 1, 1999.
Supported by DARPA/ONR under Contract No. N0014-95-0302.
Based in part on the dissertation submitted by R. W. Trice for the Ph.D. degree in materials science and engineering, The University of Michigan, Ann Arbor, MI, 1997.
*Member, American Ceramic Society.
†Now at Northwestern University, Evanston, IL.

II. Experimental Procedure

(1) Fibrous Monolith Fabrication

The methods for fabricating fibrous monolith billets have been described in detail in previous publications.[1,13–15] The basic building blocks of fibrous monoliths are small-diameter filaments (~250 μm) composed of Si_3N_4 surrounded by a thin BN layer. The thickness of the outer shell of BN is ~10–20 μm. Fibrous monoliths are composed of hundreds of filaments, giving rise to their "woodlike" architecture.

The cell material of each filament was prepared from Si_3N_4 (SN-E-10, UBE Industries, Yamaguchi, Japan) powders with 4 wt% Y_2O_3 (99.9% pure; REaction, Johnson Matthey, Ceramics, Downingtown, PA) added as a sintering aid. Hexagonal BN (HCP, Advanced Ceramics, Cleveland, OH), consisting of platelike particles 7–10 μm in diameter and 0.1–0.3 μm thick, was used to fabricate the cell boundaries in fibrous monoliths. Long, continuous filaments were manufactured by an outside vendor (Advanced Ceramics Research, Tucson, AZ) and wound onto a spool.

A filament-winding approach was used to fabricate 4Y-FMs, based on the method developed by King *et al.*[16] The uniaxially aligned filaments were warm-pressed at 150°C and 3–4 MPa, creating a 8–9 mm thick "green" billet with a high degree of filament order. A burnout step was needed to remove the polymer binder from the green billets. The billets were subjected to temperatures varying from 25° to 700°C for 98 h. As is developed in this paper, a post-binder-burnout heat treatment in air was also performed on two of the billets to remove residual carbon. Billets were hot-pressed at either 1800° or 1820°C under an applied pressure of 25 MPa for 1 h using a heating rate of 600°C/h. The load was applied when the surface temperature of the die reached 1200°C.

(2) Specimen Fabrication and Testing

The hot-pressed billets were machined to a thickness of 3 mm by removing equal amounts of material from both sides. Samples were cut from these billets using diamond blades (American Diamond Tool, Inc., Buffalo, NY) into 3 mm × 4 mm × 48 mm flexure bars. The tensile surface was always polished through 3 μm prior to testing.

The average modulus of 4Y-FM samples, determined using the acoustic resonance[17] method (Grindosonic, J. W. Lemmens, Inc., St. Louis, MO) was 295 ± 1 GPa. X-ray diffraction (XRD) of pulverized specimens revealed complete transformation of the starting α-Si_3N_4 powder to β-Si_3N_4. The point-fraction method, using a square grid, was used to estimate the volume percentage of secondary phases.

Flexure testing[18] was performed on a screw-driven load frame (Model 4483, Instron Corp., Canton, MA) equipped with a 5 kN load cell and a clamshell furnace (Applied Test Systems, Butler, PA). Material evaluations were made between 25° and 1400°C. A thermocouple was placed within 5 mm of the sample (and near the mid-span) during testing. A 10 min dwell at ±2°C of the desired testing temperature was achieved before testing. A SiC fixture, with outer and inner spans fixed at 40 and 20 mm, respectively, was used for all tests. All

Table I. Overview of Processing Trials in the Development of 4Y-FMs

Billet	Post-binder-burnout heat treatment	Melilite observed	Hot-press temperature (°C)	Relative cell-boundary strength	Cell-boundary glassy phase (vol%)	Density (g/cm^3)
4Y-FM-1	No	Yes	1800	Weak	Not measured	3.01 ± 0.01
4Y-FM-2	Yes	No	1800	Weak	7 ± 1.5	3.04 ± 0.01
4Y-FM-3	Yes	No	1820	Strong	12 ± 2.3	3.04 ± 0.01

flexural tests were conducted at a rate of 0.5 mm/min. The work of fracture of each specimen was calculated by determining the area under the load–crosshead deflection curve and dividing it by twice the cross-sectional area of the sample. An apparent stress was calculated using load and the original cross-sectional area, employing the standard specified equation for stress in 4-point loading.

III. Results and Discussion

(1) Processing Trials of 4Y-FMs

An overview of the billets fabricated for this study is shown in Table I. Two problems arose during the early attempts to fabricate fibrous monoliths using 4 wt% Y_2O_3 sintering aids. These were (1) formation of melilite, $Y_2O_3{\cdot}Si_3N_4$, a secondary phase subject to extreme oxidation near 1000°C, and (2) weak BN cell boundaries. The origin and resolution of these two problems are discussed presently.

(A) Formation of the Melilite Phase: Billet 4Y-FM-1 was hot-pressed at 1800°C for 1 h. Density measurements[19] averaged 99.1% of the theoretical density of 3.04 g/cm^3 for this composition of fibrous monolith (assuming 80 vol% Si_3N_4 cells and 20 vol% BN cell boundaries). XRD of pulverized samples, shown in Fig. 1, indicated the presence of β-Si_3N_4, *h*-BN, and $Y_2O_3{\cdot}Si_3N_4$, commonly referred to as melilite.

Melilite, a quaternary phase formed by the reaction of Si_3N_4 and Y_2O_3, was originally thought to be highly refractory. However, early researchers did not realize that while the melilite phase is very refractory[20] at 1400°C, it undergoes severe oxidation in the 900°–1100°C temperature range because of the large stresses that develop in the surface scale during oxidation.[21] The reaction equation is[22]

$$Y_2O_3{\cdot}Si_3N_4 + 3O_2 \rightarrow Y_2Si_2O_7 + SiO_2 + 2N_2 \quad (1)$$

where melilite transforms to yttrium silicate and cristobalite. The specific volume increase associated with this reaction is ~30%. As a result of the volume change, the oxidation product does not form a protective layer on the surface of the Si_3N_4, but cracks instead, exposing new unoxidized Si_3N_4. This process continues until complete failure occurs.

Figure 2 presents the phase diagram for Si_3N_4–Y_2O_3–SiO_2. Starting powders that would fix compositions in the Si_3N_4–$Y_2O_3{\cdot}Si_3N_4$–$YSiO_2N$ region (triangle I) are to be avoided because of the formation of melilite. The Si_3N_4–$Y_2Si_2O_7$–Si_2N_2O region (triangle II) is more desirable, because the reaction products demonstrate excellent oxidation resistance.[21] From the phase diagram, ~2.4 wt% SiO_2 is required to put the reaction products in compatibility triangle II.[23] Because 3 wt% SiO_2 exists in this Si_3N_4 powder, melilite should not be formed during hot-pressing.[24] However, the diffraction pattern in Fig. 1 shows that this is not the case.

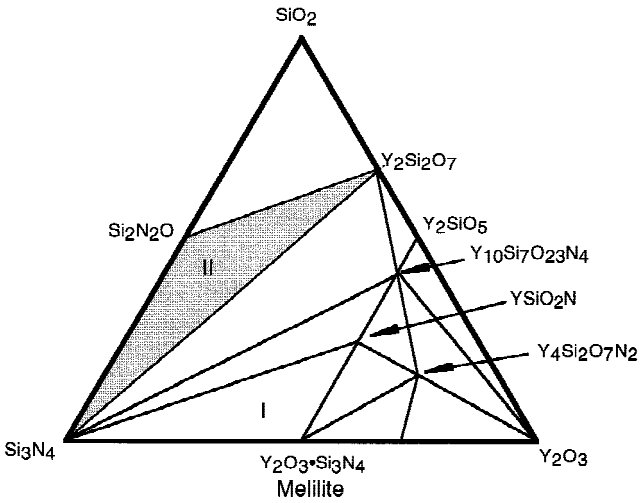

Fig. 2. Phase diagram for the Si_3N_4–Y_2O_3–SiO_2 system. Shaded region (II) is the desired reaction product composition triangle to avoid formation of either melilite or other quaternary phases.

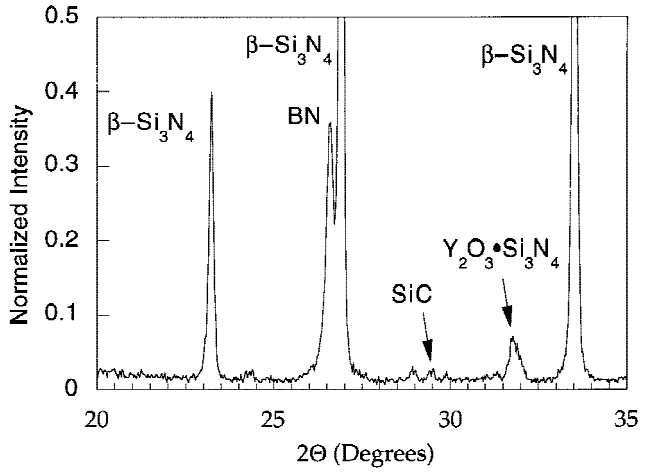

Fig. 1. XRD results of billet 4Y-FM-1. Presence of melilite, $Y_2O_3{\cdot}Si_3N_4$, was observed. Intensity was normalized to β-Si_3N_4 at $2\theta = 27°$.

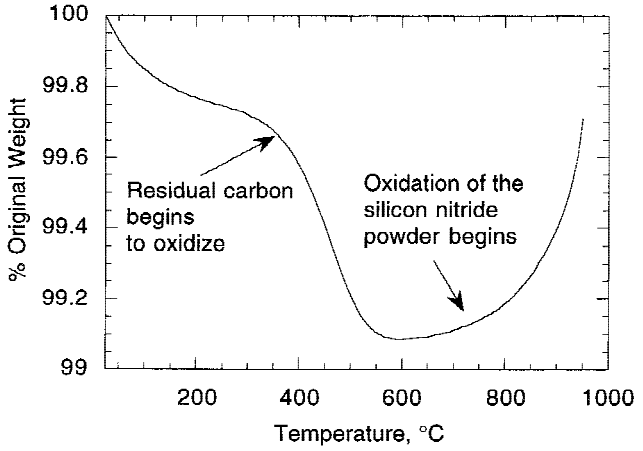

Fig. 3. Thermogravimetric response of a ceramic powder/residual carbon sample heated in flowing air from room temperature through 900°C. Sharp decrease in weight beginning near 400°C is due to oxidation of residual carbon.

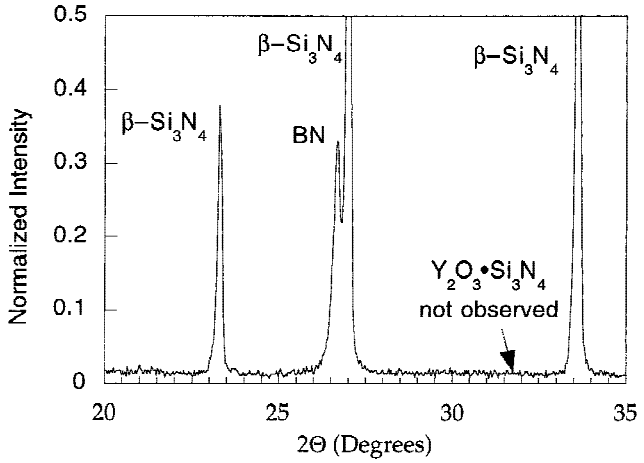

Fig. 4. XRD results from a sample taken from 4Y-FM-2. This billet was subject to a post-binder-burnout heat treatment in air before hot-pressing to remove residual carbon. No melilite was observed. (Intensity was normalized to β-Si_3N_4 at $2\theta = 27°$.)

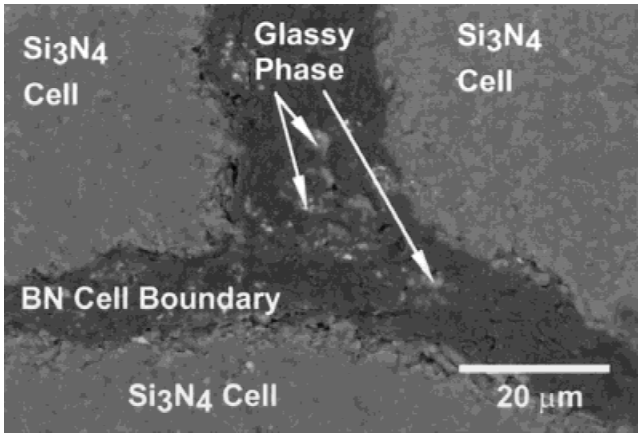

Fig. 6. Backscattered SEM image from 4Y-FM-2 indicating a typical cell boundary created at the intersection of three Si_3N_4 cells. Bright phase is the cell-boundary glassy phase and is a result of sintering aid migration from the cells of the Si_3N_4 to the BN cell boundary during hot-pressing.

One of the consequences of using polymers during the fabrication of fibrous monoliths is the residual carbon concentration after binder burnout in flowing nitrogen. Hampshire and Jack[25] showed that when Y_2O_3-doped Si_3N_4 is hot-pressed, the final products are dependent upon the initial oxygen and carbon concentrations. The carbon reacts with the SiO_2 present on the Si_3N_4 powder according to:

$$SiO_2 + C \rightarrow SiO + CO \quad (2)$$

where the SiO_2 concentration needed to avoid formation of melilite is vaporized. Thus, it appears that the carbon leftover after binder burnout is reacting with the surface SiO_2 during hot-pressing, depleting the Si_3N_4 powders of SiO_2 and forming melilite.

To evaluate this hypothesis, the residual concentration of carbon was significantly reduced before hot-pressing by a post binder-burnout heat treatment in air. Figure 3 shows the results of a thermogravimetric test, conducted in flowing air, used to establish the temperature where carbon was oxidized. The test sample was taken from a billet after a typical binder burnout run in nitrogen and was composed of ~99.2 wt% ceramic powder and ~0.8 wt% residual carbon. Upon heating, there was an initial weight loss of 0.3 wt% that was likely the result of absorbed moisture in the sample. The sharp decline in weight observed near 400°C and continued through 550°C was due to oxidation of the residual carbon. The weight of the sample began to increase beyond 700°C, indicating that oxidation of the powders was occurring. Based on these results, a post binder-burnout schedule was developed that included a 24 h dwell at 400°C in flowing air.

A second fibrous monolith billet, 4Y-FM-2, was fabricated by inserting the post binder-burnout treatment between the binder burnout and hot-pressing steps. The residual carbon concentration was found to be 0.13 ± 0.01 wt% following this post binder-burnout treatment. Following this additional process step, this billet was hot-pressed under identical conditions as 4Y-FM-1. None of the deleterious melilite was observed in XRD patterns of a sample from 4Y-FM-2, as shown in Fig. 4.

(B) Weak Cell Boundaries in 4Y-FM Billets: A fully dense 4 wt% Y_2O_3 *monolithic* Si_3N_4 billet was fabricated using a 1 h hot-press at 1800°C and 25 MPa. Based on this understanding, identical hot-pressing conditions were used to fabricate 4Y-FM-2. The average density of this billet was 3.04 g/cm^3, equivalent to the theoretical density. However, this billet was not structurally sound, because it was easy to flake off individual cells of Si_3N_4. Figure 5(a) shows the results of a flexure test run at 25°C on a sample machined from this billet. Based on the flexural response and observations of the failed sample, it was deduced that shear-initiated failure occurred at the midplane of the specimen. Failure analysis revealed that the initial crack originated in the BN cell boundary, an indication that the cell boundary was very weak compared with the strength of the cells.

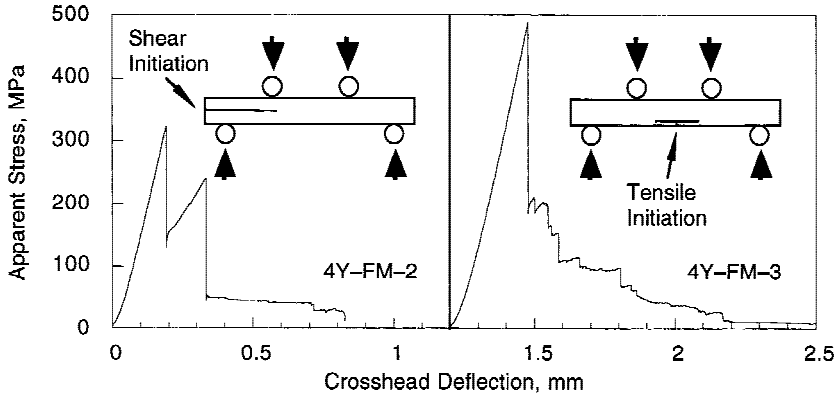

Fig. 5. Comparison of the 25°C flexural response of samples cut from 4Y-FM-2 and 4Y-FM-3. Shear failure occurred, initiated within the weak BN cell boundary, near the midplane of the sample in the billet hot-pressed at the lower temperature (1800°C). Tensile failure, initiated within the Si_3N_4 cells, was observed in the billet hot-pressed at the higher temperature (1820°C).

Table II. Comparison of Flexure Strength for Two Fibrous Monoliths†

Temperature (°C)	Fibrous monolith composition	Strength (MPa)	Work of fracture (J/m^2)
25	6Y/2Al-FM	510 ± 87	7400 ± 1350
	4Y-FM-3	553	6700
1000	6Y/2Al-FM	440 ± 110	7800 ± 2100
	4Y-FM-3	390	4800
1400	6Y/2Al-FM	176	3200
	4Y-FM-3	293	3000

†Different compositions of sintering aids added to the Si_3N_4 cells.[27]

Billet 4Y-FM-3 was fabricated at an increased hot-pressing temperature of 1820°C. Like 4Y-FM-2, samples cut from billet 4Y-FM-3 exhibited theoretical densities. However, it was not possible to flake off individual cells of Si_3N_4 from the surface, suggesting a stronger cell boundary. Figure 5(b) presents the 25°C flexure results for a sample cut from 4Y-FM-3. The stress versus crosshead deflection curve and fractured specimen both indicated that failure initiated on the tensile surface in the Si_3N_4 cells.

The presence of a secondary phase in the BN is the likely reason for the stronger cell boundaries displayed by 4Y-FM-3. Previous research[26] has shown that the sintering aid glass formed in the Si_3N_4 cells flows into the BN cell boundaries during hot-pressing and resides there upon cooling. An example of the cell-boundary glassy phase is shown in Fig. 6, a backscattered SEM image of a cross section of a 4Y-FM-2 sample near the intersection of three cells. A bright phase, previously shown to have the same composition as the residual glassy phase between the grains of Si_3N_4, is clustered at the intersection of the three filaments.[26] Cross-sectional analysis of samples cut from 4Y-FM-2 indicates the amount of glassy phase present in the cell boundary is relatively low, only 7 ± 1.5 vol%. A 12 vol% glass is measured in the cell boundary of 4Y-FM-3. Thus, increasing the hot-pressing temperature has increased the amount of glassy phase that has flowed into the BN cell boundary during processing. The increased amount of glass in the cell boundary seems to have increased its strength, so that failure is now favored first in the Si_3N_4 cells rather than in the BN cell boundary.

(2) Effect of Sintering Aid Composition on the Mechanical Properties of Si_3N_4/BN Fibrous Monoliths

The following section addresses the effect of varying sintering aid composition on the high-temperature mechanical properties of fibrous monoliths. The mechanical results of 4Y-FM-3 are compared to a less-refractory fibrous monolith,[27] in which the sintering aids added to the Si_3N_4 cells are 6 wt% Y_2O_3 and 2 wt% Al_2O_3. Samples cut from these billets are designated as 6Y/2Al-FMs and represent a composition of fibrous monoliths that have been extensively studied. Previous research indicated that Al_2O_3 additions to Y_2O_3-doped Si_3N_4 decreased its flexure strength at elevated temperatures.[7] Table II lists the results of the flexure tests. The mechanical behavior of 6Y/2Al-FMs is compared to individual samples from 4Y-FM-3. Because of the limited number of specimens, the discussion focuses on failure modes and load–deflection response.

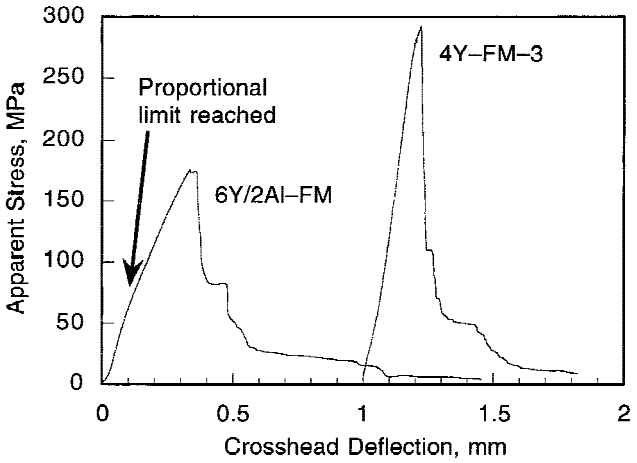

Fig. 8. Flexural response comparison of a 4Y-FM-3 and 6Y/2Al-FM tested at 1400°C. Proportional limit was reached at only 65 MPa for the 6Y/2Al-FM.

(A) Effect of Sintering Aid Composition at 25°C: The 25°C flexural response of the two compositions of fibrous monoliths was very similar. Figure 7 presents a side view of 4Y-FM-3 after testing. The fracture behavior is similar to that observed in 6Y/2Al-FMs.[1] As expected, varying the sintering aid composition seems to have little effect on the room-temperature mechanical properties of fibrous monoliths.

(B) Effect of Sintering Aid Composition at 1000°C: The flexural response and microscopic investigations of both compositions of fibrous monoliths tested at 1000°C indicated that tensile-initiated failure was observed in 6Y/2Al-FMs, while shear-initiated failure was observed in the 4Y-FM sample. The difference in failure mode was a consequence of the smaller amount of cell-boundary glassy phase present in 4Y-FM-3 as compared with 6Y/2Al-FMs. 6Y/2Al-FMs contained 19 vol% cell-boundary glassy phase compared to 12 vol% for 4Y-FMs. The general trend observed when shear-initiated failure is favored over tensile-initiated failure is a reduction in the overall strength of the sample. Thus, shear failure is to be avoided by having sufficient glassy phase (>16–18 vol%) in the BN cell boundaries.

(C) Effect of Sintering Aid Composition at 1400°C: The characteristic stress–deflection curves for specimens of both sintering aid compositions tested at 1400°C are presented in Fig. 8. It is evident that the 6Y/2Al-FM sample exhibits nonlinear stress–deflection behavior at 65 MPa, well before tensile

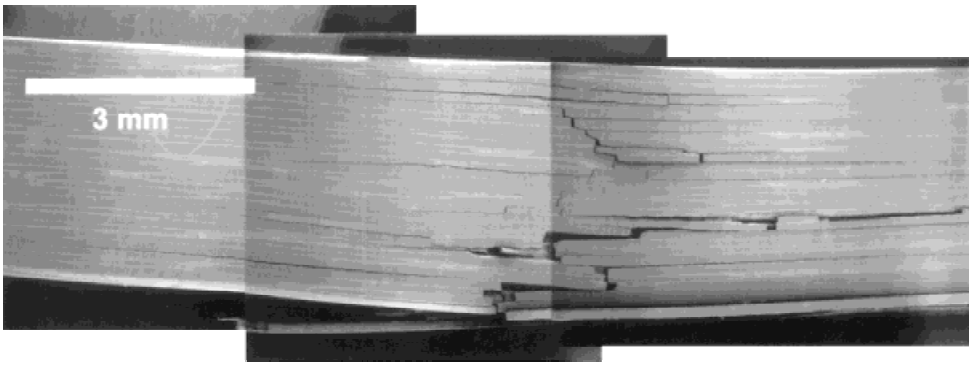

Fig. 7. Side view of a 4Y-FM-3 flexure sample tested at 25°C. Its failure response was similar to that of 6Y/2Al-FMs tested at 25°C.

fracture initiates in the Si_3N_4 cells. The fibrous monolith made with 4 wt% Y_2O_3 is linear elastic to 280 MPa before failing from tensile-initiated cracks in the cells. This response is expected in 4Y-FMs, because the glassy phase formed from the sintering aids (as manifested in the Si_3N_4 cells) is more refractory.

IV. Conclusions

A completely dense, 4-wt%-Y_2O_3–Si_3N_4/BN fibrous monolith has been fabricated in an effort to improve the high-temperature properties of fibrous monoliths. At 1400°C, the 4Y-FM exhibited elastic behavior through 280 MPa, whereas considerable nonlinear loading behavior was observed in the less-refractory-composition fibrous monolith.

The presence of residual carbon following binder burnout was found to be responsible for the formation of $Y_2O_3{\cdot}Si_3N_4$, a phase known to undergo severe oxidation between 900° and 1100°C. XRD results indicated that $Y_2O_3{\cdot}Si_3N_4$ was not formed during hot-pressing if residual carbon was removed prior to hot-pressing with an additional binder-burnout processing step at 400°C in air. Furthermore, the small volume percentage of sintering aids used limited the amount of sintering aid glass that migrated to the cell boundary during hot-pressing, resulting in fibrous monoliths with extremely weak cell boundaries. Increasing the hot-press temperature by 20°C, to 1820°C, resulted in an increased percentage of glassy phase in the cell boundary and, thus, stronger cell boundaries.

Ultimately, increasing the refractoriness of the glassy phase by adjusting the starting sintering aid composition improves the high-temperature performance of fibrous monoliths at 1400°C. The problem is that increasing the refractoriness of the Si_3N_4 often involves using *less* sintering aid. The result is that less glassy phase is available to migrate into the cell boundary during hot-pressing. This favors shear initiation at temperatures <1400°C, which can significantly reduce the strength of a fibrous monolith in the intermediate temperature ranges (1000°–1300°C).

References

[1]D. Kovar, B. H. King, R. W. Trice, and J. W. Halloran, "Fibrous Monolithic Ceramics," *J. Am. Ceram. Soc.*, **80** [10] 2471–87 (1997).

[2]R. L. Tsai and R. Raj, "Creep Fracture in Ceramics Containing Small Amounts of a Liquid Phase," *Acta Metall.*, **30**, 1043–58 (1982).

[3]M. D. Thouless, "A Review of Creep Rupture in Materials Containing an Amorphous Phase," *Res. Mech.*, **22**, 213–42 (1987).

[4]D. R. Clarke and G. Thomas, "Grain Boundary in a Hot-Pressed MgO Fluxed Silicon Nitride," *J. Am. Ceram. Soc.*, **60** [11–12] 491–95 (1977).

[5]L. K. V. Lou, T. E. Mitchell, and A. H. Heuer, "Impurity Phases in Hot-Pressed Si_3N_4," *J. Am. Ceram. Soc.*, **61** [9–10] 392–96 (1978).

[6]D. W. Richerson, "Effect of Impurities on the High-Temperature Properties of Hot-Pressed Silicon Nitride," *Am. Ceram. Soc. Bull.*, **52** [7] 560–62, 569 (1973).

[7]A. E. Pasto, W. C. Van Schalkwyk, and F. M. Mahoney, "Creep Behavior of Yttria- and Alumina-Doped Silicon Nitride"; pp. 776–85 in *Ceramic Materials and Components for Engines*, Proceedings of the 3rd International Symposium on Ceramic Materials and Components for Engines (Las Vegas, NV, Nov. 1988). Edited by V. Tennery. American Ceramic Society, Westerville, OH, 1989.

[8]G. E. Gazza, "Effect of Yttria Additions on Hot-Pressed Si_3N_4," *Am. Ceram. Soc. Bull.*, **54** [9] 778–81 (1975).

[9]W. E. Luecke, S. M. Wiederhorn, B. J. Hockey, R. F. Krause, Jr., and G. G. Long, "Cavitation Contributes Substantially to Tensile Creep in Silicon Nitride," *J. Am. Ceram. Soc.*, **78** [8] 2085–96 (1995).

[10]D. C. Cranmer, B. J. Hockey, S. M. Wiederhorn, and R. Yeckley, "Creep and Creep Rupture of HIP'ed Si_3N_4," *Ceram. Eng. Sci. Proc.*, **12** [9–10] 1862–72 (1991).

[11]M. K. Ferber and M. G. Jenkins, "Evaluation of the Strength and Creep–Fatigue Behavior of Hot Isostatically Pressed Silicon Nitride," *J. Am. Ceram. Soc.*, **75** [9] 2453–62 (1992).

[12]C. J. Gadaska, "Tensile Creep in an *In Situ* Reinforced Silicon Nitride," *J. Am. Ceram. Soc.*, **77** [9] 2408–18 (1994).

[13]S. Baskaran and J. W. Halloran, "Fibrous Monolithic Ceramics: II, Flexural Strength and Fracture Behavior of the Silicon Carbide/Graphite System," *J. Am. Ceram. Soc.*, **76** [9] 2217–24 (1993).

[14]G. Hilmas, A. Brady, U. Abdali, G. Zywicki, and J. Halloran, "Fibrous Monoliths: Non-brittle Fracture from Powder-Processed Ceramics," *Mater. Sci. Eng. A*, **195**, 263–68 (1995).

[15]G. E. Hilmas, G. A. Brady, and J. W. Halloran, "SiC and Si_3N_4 Fibrous Monoliths: Nonbrittle Fracture from Powder-Processed Ceramics Produced by Coextrusion"; pp. 609–14 in Ceramic Transactions, Vol. 51, *Fifth International Conference on Ceramic Processing Science and Technology*. Edited by H. Hausner, G. L. Messing, and S.-I. Hirano. American Ceramic Society, Westerville, OH, 1994.

[16]B. H. King, "The Influence of Architecture on the Elasticity and Strength of Si_3N_4/BN Fibrous Monolithic Ceramic Laminates"; Ph.D. thesis. University of Michigan, Ann Arbor, MI, 1997.

[17]"Standard Test Method for Dynamic Young's Modulus Shear Modulus, and Poissons Ratio for Advanced Ceramics by Sonic Resonance," ASTM Designation C1198–96. American Society for Testing and Materials, West Conshohocken, PA.

[18]MIL-STD-1942, "Flexural Strength of High Performance Ceramics at Ambient Temperatures," Nov. 1990.

[19]Standard Test Method for Water Absorption, Bulk Density, Apparent Porosity, and Apparent Specific Gravity of Fired Whiteware Products," ASTM Designation C373–88. American Society for Testing and Materials, West Conshohocken, PA.

[20]A. Tsuge, K. Nishida, and M. Komatsu, "Effect of Crystallizing the Grain-Boundary Glass Phase on the High-Temperature Strength of Hot-Pressed Si_3N_4 Containing Y_2O_3," *J. Am. Ceram. Soc.*, **58** [7–8] 323–26 (1975).

[21]F. F. Lange, S. C. Singhal, and R. C. Kuznicki, "Phase Relations and Stability Studies in the Si_3N_4–SiO_2–Y_2O_3 Pseudoternary System," *J. Am. Ceram. Soc.*, **60** [5–6] 249–52 (1977).

[22]S. Hampshire, "Nitride Ceramics"; pp. 119–70 in Material Science and Technology: A Comprehensive Treatment, Vol. 11, *Structure and Properties of Ceramics*. Edited by R. W. Cahn, P. Haasen, and E. J. Kramer. VCH, Weinheim, Germany, 1994.

[23]S. Natansohn, A. E. Pasto, and W. J. Rourke, "Effect of Powder Surface Modifications on the Properties of Silicon Nitride Ceramics," *J. Am. Ceram. Soc.*, **76** [9] 2273–84 (1993).

[24]M. Pueckert and P. Greil, "Oxygen Distribution in Silicon Nitride Powders," *J. Mater. Sci.*, **22**, 3717–20 (1987).

[25]S. Hampshire and K. H. Jack, *Ceramic Components for Engines*; pp. 350–57. Edited by S. Sō miya, E. Kanai, and K. Ando. KTK Scientific, Tokyo, Japan, 1984.

[26]R. W. Trice and J. W. Halloran, "Influence of Microstructure and Temperature on the Interfacial Fracture Energy Silicon Nitride/Boron Nitride Fibrous Monolithic Ceramics," *J. Am. Ceram. Soc.*, **82** [9] 2502–508 (1999).

[27]R. W. Trice and J. W. Halloran, "Elevated Temperature Mechanical Properties of Silicon Nitride/Boron Nitride Fibrous Monolithic Ceramics," *J. Am. Ceram. Soc.*, in press. □